Simulation of Acoustic Energy Harvesting Using Piezoelectric Plates in a Quarter-wavelength Straight-tube Resonator

Bin Li and Jeong Ho You*
Department of Mechanical Engineering, Southern Methodist University, Dallas, TX, USA
*Corresponding author: Department of Mechanical Engineering, Southern Methodist University, Dallas, TX, 75205, USA, jyou@smu.edu

Abstract: An acoustic energy harvesting mechanism at low frequency (~200 Hz) using lead zirconate titanate (PZT) piezoelectric cantilever plates placed inside a quarter-wavelength straight-tube resonator has been studied numerically using COMSOL *Multiphysics* 4.3 and compared with experimental data. When the tube resonator is excited by an incident wave at its acoustic eigenfrequency, an amplified acoustic resonant wave is developed inside the tube and drives the vibration motion of the piezoelectric plates. When a single piezoelectric plate is placed inside the tube, the plate displacement and output voltage gradually decrease as it moves from the tube open inlet to the tube closed end. When multiple piezoelectric plates are placed inside the tube resonator, the interaction between air particle motion and piezoelectric plates plays an important role in determining the amount of harvested acoustic power. The calculated results of output voltage and power of the piezoelectric plates match well with experimental data.

Keywords: Acoustic energy harvesting, piezoelectric cantilever plate, quarter-wavelength resonator.

1. Introduction

Harvesting mechanical vibration energy via piezoelectric materials has been widely studied numerically using COMSOL *multiphysics*. Kamel *et al.* [1] used beam bending theory to predict the generated electric power from vibrational piezoelectric harvesting devices (PHD). Renaud *et al.* [2] proposed design and characterization of a prototype of a piezoelectric bending harvester to scavenge energy from motion of human limbs. Majidi *et al.* [3] applied an array of vertically aligned zinc oxide (ZnO) nanoribbons to harvest nanoscale vibrational energy. Wang *et al.* [4] used a curved beam in the cavity of a sonic crystal to harvest acoustic energy. Zurkinden *et al.* [5] investigated the harvesting mechanism of ocean surface wave energy using PVDF films. Kuehne *et al.* [6] studied a piezoelectric harvesting micro generator for a tire pressure monitoring wireless sensor node. The performance of piezoelectric micro-power generators has been calculated numerically using COMSOL, ANSYS, and CoventorWare [7].

Acoustic energy is clean, ubiquitous, and sustainable in our life, so it is a good candidate for an alternative energy resource. There are a few simulation and experimental studies to develop acoustic energy harvesting mechanisms using piezoelectric transducers in the recent years [4, 8-10]. However, most previous studies have focused on harvesting at relatively high frequencies (a few kHz or MHz), which is rarely available in everyday life.

In this study, we have performed numerical simulations of an acoustic energy harvester which consists of a quarter-wavelength straight-tube resonator and piezoelectric cantilever plates placed inside the tube using COMSOL *Multiphysics* 4.3. The length of tube is designed to have a low operating frequency of ~200 Hz. Inside the tube resonator, single and multiple lead zirconate titanate (PZT) piezoelectric plates are placed to convert acoustic resonant energy to electricity. The simulation results are compared with the experimental data.

2. Acoustic resonator

Acoustic resonators such as Helmholtz resonator, half-wavelength, and quarter-wavelength resonators have been widely used for both sound augmentation and noise attenuation. A typical Helmholtz resonator (HR) consists of a neck and a cavity. When the frequency of the incident sound wave matches with the first eigenfrequency of HR, the air in the neck oscillates as a mass while the static air in the cavity undergoes compression and expansion as a spring. With the sound radiation from the neck inlet as a damper, HR can be modeled as a mass-

spring-damper system as shown in Fig. 1. The mode shapes, eigenfrequencies, amplification factor, and transmission characteristics of HR have been studied successfully using COMSOL [9, 11, 12] and the simulation results match well with the analytical solutions based on lumped elements [9].

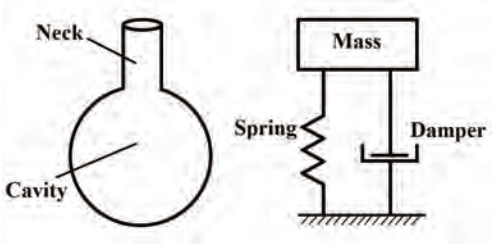

Figure 1. Sketch of Helmholtz resonator.

Unlike the Helmholtz resonator, a quarter-wavelength resonator cannot be modeled as lumped elements because its longitudinal dimension is not much smaller than the wavelength. It has been experimentally proved that a quarter-wavelength resonator requires less volume than HR to collect the same amount of acoustic energy at a given frequency [13]. Also, a quarter-wavelength resonator collects acoustic energy about three times more than a half-wavelength resonator [13]. Therefore, a quarter-wavelength resonator is expected to be the best design to collect acoustic energy in a closed space.

Firstly, eigenfrequency calculation in COMSOL is used to describe the resonant behavior of a quarter-wavelength straight-resonator. The quarter-wavelength resonator is 42 cm long with 4cm×5cm rectangular cross-section as shown in Fig. 2 (a). In eigenfrequency calculation, the tube inlet is set as sound soft and the other boundaries are set as sound hard.

As shown in Fig. 2 (b), the normalized acoustic pressure p_n ($p_n=p/p_{max}$) and the normalized acoustic pressure gradient ∇p_n ($\nabla p_n=\nabla p/\nabla p_{max}$) along the longitudinal z direction of the tube resonator at the first resonant mode can be represented as sinusoidal functions [14]

$$p_n(z) = \sin\frac{\pi z}{2L}, \quad (1)$$

$$\nabla p_n(z) = \cos\frac{\pi z}{2L}. \quad (2)$$

where L is the tube length equal to a quarter wavelength. Clearly, p_n increases sinusoidally from the tube inlet to the end while ∇p_n shows the opposite trend.

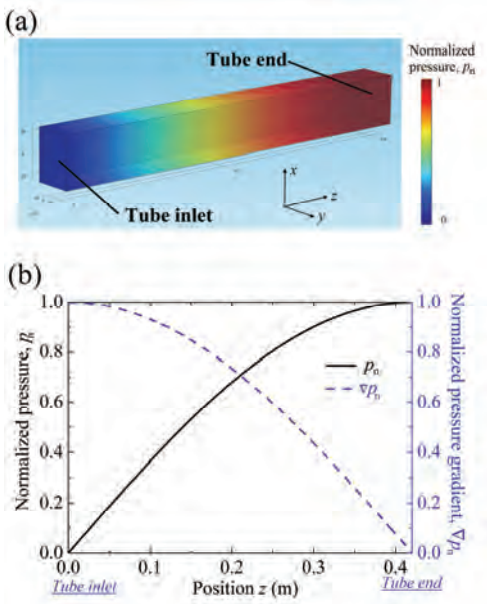

Figure 2. (a) First eigenmode shape of a 42 cm long quarter-wavelength tube resonator and (b) normalized pressure and normalized pressure gradient along the tube longitudinal z direction.

In order to convert the acoustic energy to electricity, piezoelectric plates are placed inside the tube resonator as shown in Fig. 3 (a). The structural eigenfrequency of the piezoelectric plates are designed to be same as the acoustic resonant frequency of the tube to maximize the harvested energy. When the tube resonator is excited by an incident wave at its acoustic eigenfrequency, the amplified standing wave is developed inside the tube resonator. Then, the pressure difference Δp between each side of the plates drive the vibration motion of the piezoelectric plates and generate electricity by the d_{31} mode. Fig. 3 (b) and (c) show the eigenmode shape and normalized pressure of the quarter-wavelength tube resonator with three piezoelectric plates placed inside. The first eigenmode shape of the tube still follows the sinusoidal function from Eq. (1). However, there is pressure discontinuity at the position of plates. The pressure differences $\Delta p_n i$ (i=1, 2 and 3) are the driving force for the piezoelectric plate motion. It can be found that $\Delta p_n 1 > \Delta p_n 2 > \Delta p_n 3$,

indicating that the driving forces decrease gradually when the plate moving from the tube inlet to the tube end.

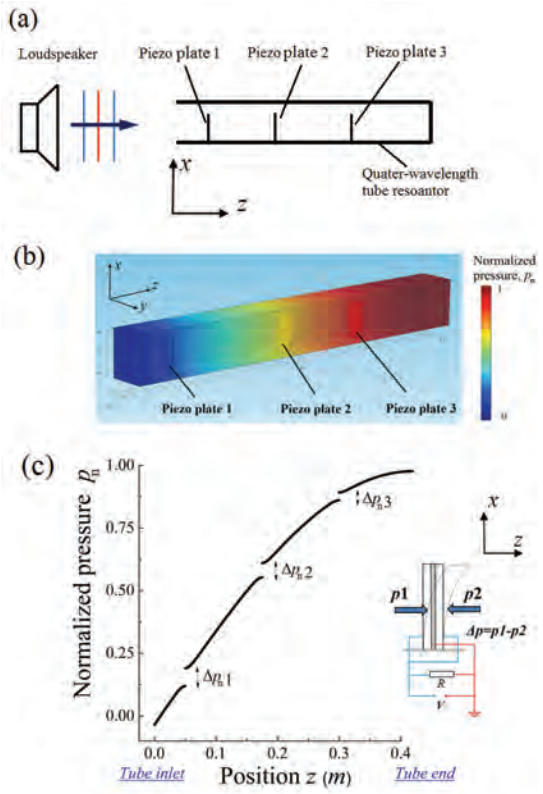

Figure 3. (a) Sketch of acoustic energy harvesting using piezoelectric cantilever plates in a quarter-wavelength tube resonator, (b) the eigenmode shape of the 42 cm quarter-wavelength tube resonator when three piezoelectric plates placed inside and (c) the normalized pressure along the tube longitudinal direction of tube resonator with three piezoelectric plates.

3. Use of COMSOL Multiphysics

The 3D pressure acoustics, solid mechanics, and piezoelectric devices modules in COMSOL *multiphysics* 4.3 are combined to calculate the output voltage and power in frequency domain. The 42 cm long tube is made of 1/2 inch thick polycarbonate plates and the dimensions of PZT piezoelectric plates are 2×4×0.07 cm. The structure and materials properties of PZT piezoelectric plates and polycarbonate blocks are provided in Table 1.

Table 1: Structure and material properties of PZT piezoelectric plate and polycarbonate.

Type	Symbol	Value
Piezo plate size		
Height	l	4 cm
Width	b	2 cm
Total thickness	t	0.7 mm
Piezo plate structure		
PZT layers	t_p	0.48 mm
Carbon fiber	t_c	0.22 mm
Piezo plate's capacitance	C_p	75 nF
PZT's Piezo constant	d_{31} d_{33}	750 pC/N -320 pC/N
PZT relatively permittivity	$\varepsilon/\varepsilon_0$	4500
PZT Young's modulus	E_p	40 GPa
PZT density	ρ_p	7400 kg/m^3
PZT damping ratio	ζ	0.025
Carbon fiber's Young's modulus	E_c	2 GPa
Polycarbonate's density	ρ_p	1175 kg/m^3
Polycarbonate's Young's modulus	E_{pc}	2.2 GPa

3.1 Governing equations

The strain-charge form constitutive equation of the piezoelectric materials is:

$$\{D\} = [d]\{T\} + [\varepsilon^T]\{E\}, \quad (3)$$

where $\{T\}$ is the vector of the stresses, $\{D\}$ is the electric displacement vector, $\{E\}$ is the electric field vector, $[d]$ is a 3×6 matrix of piezoelectric constant, $[\varepsilon^T]$ is a 3×3 dielectric constant matrix. When the cantilever piezoelectric plate is bended by Δp, the longitudinal bending stress (T_{xx}) would be converted to electrical potential V along the thickness direction by the piezoelectric d_{31} mode, see Fig. 3 (c).

Output power harvested by piezoelectric materials strongly depends on the impedance of external circuit. The output power and the optimized loading resistance of a piezoelectric generator have been derived for the base excitation [15]. In a similar manner, the output electric power P of a piezoelectric cantilever plate vibrated by an external pressure difference Δp can be expressed as

$$P = \frac{(\omega_n dt_p/\varepsilon)^2 RC_p{}^2}{(\omega_n R^2 C_p{}^2(4\zeta^2+k^4)+4\zeta^2+4k^2\zeta\omega_n RC_p} \times (\frac{t_c l^2 b}{6I}\Delta p)^2, \quad (4)$$

where k is the piezoelectric coupling coefficient, d is the piezoelectric constant, C_p is the piezoelectric capacitance, R is the external loading resistance, ε is the permittivity, ζ is the damping ratio, t_p is the thickness of piezoelectric material, t_c is the thickness of center shim (carbon fiber in this study), ω_n is the structural eigenfrequency of the piezoelectric plate, l is the length of the plate, b is the width of the plate, and I is the moment of inertia. The optimized external resistance can be obtained when $\partial P/\partial R=0$

$$R = \frac{1}{\omega_n C_p}\frac{2\zeta}{\sqrt{4\zeta^2+k^4}}. \quad (5)$$

3.2 Geometry

As shown in Fig. 4 (a), the background pressure is used to generate a plane wave along z direction in a semisphere with a diameter of 1.68 m (one wavelength). The 42 cm long rectangular tube is placed along z direction. At the resonance of tube, the air motion near the inlet generates the sound radiation in a radial direction outward from the tube inlet. In order to minimize the reflection of the radiated sound, a semispherical PML layer with a diameter of 5.04 m (three wavelengths) is used to surround the background pressure domain. The 2×4×0.07 cm^3 rectangular PZT clamped-free cantilever piezoelectric plates are placed along the centerline of the tube resonator.

3.3 Submodel

The parallel bimorph PZT plate is composed of two PZT layers and one carbon fiber layer, as shown in Fig. 4 (d). Total thickness of the piezoelectric plate is only 0.7 mm. Also, the piezoelectric layer is only 0.48 mm thick and the carbon fiber is 0.22 mm thick, which are much smaller compared to the tube resonator and the global model. It would bring difficulties in meshing and significantly increase the calculation time. To resolve this issue, we have used a submodel method. The piezoelectric plate is firstly defined in solid mechanics module as a linear elastic solid block in the global model. In the global model, the displacement of elastic solid block induced by the acoustic resonant wave is calculated and saved. Secondly, an accurate piezoelectric plate is created containing all layers in piezoelectric devices modulus. To derive the vibration motion of the piezoelectric plate, the calculated displacement from the global model is used as boundary conditions. Then, the output voltage of the piezoelectric plate can be calculated.

3.4 Boundary conditions

The background pressure field is applied to generate a travelling plane wave. A PML layer is used to absorb the radiation from the tube inlet. The interface between the PML and background pressure field is set as far-field calculation. The background acoustic pressure blows into the tube resonator which is surrounded by an acoustic cylinder domain with 0.84 m in diameter and 2 m in length. Besides, the most outer boundaries of the global model are set as a radiation boundary to minimize the reflection back into the system. Material properties and thickness of polycarbonate tube are also included in the simulations to consider sound leakage through tube wall materials.

In the submodel, as shown in Fig. 4 (d), the surfaces of piezoelectric plate are defined as a floating potential. The carbon fiber is connected to the ground. Therefore, the generated voltage will be along the thickness direction.

3.5 Mesh and solver

All domains are meshed by Free Tetrahedral elements except piezoelectric plate domains. The piezoelectric plate domains are divided in 5 element layers along the thickness direction by a sweep mesh. The sweep mesh is also applied in the submodel to create 5 elements layer per material layer along the thickness direction. When 8 piezoelectric plates placed inside the tube resonator, the global model is composed of 118, 430 elements.

Both of global model and submodel are solved in frequency domain. The solvers are chosen for MUMPS.

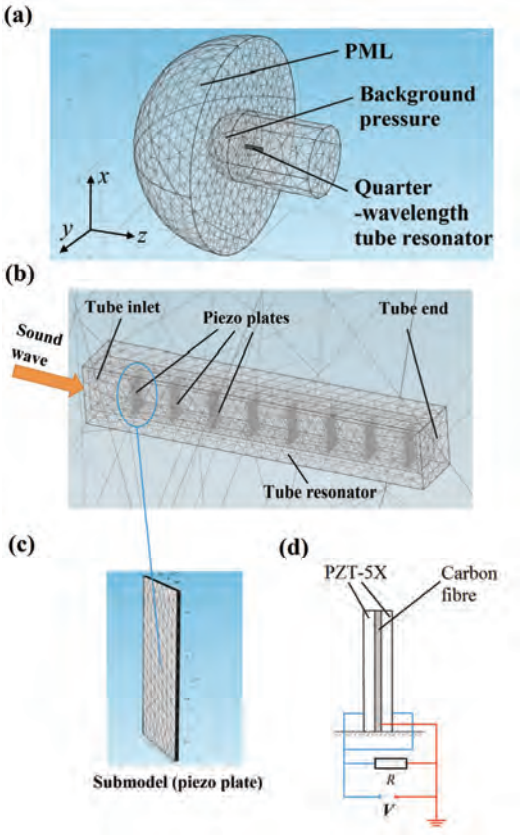

Figure 4. (a) Global model, (b) tube resonator with 8 piezoelectric plates placed inside, (c) submodel for piezoelectric plate and (d) structure and circuit connection for the parallel bimorph piezoelectric plate.

4. Experiment setup

JBL JRX118S 18 inch Compact Subwoofer driven by Crown XLS 1000 DriveCore Series power amplifier is used to generate an incident sound wave 100 dB. Quarter-inch condenser microphones (377C10 by *PCB Piezotronics*) are used to measure the acoustic amplification factor. Parallel bimorph PZT plates (model Stripe Actuator 40-2010 manufactured by *APC International, Ltd.*) have been chosen to harvest the acoustic energy. A data acquisition system (DAQ) NI-PCI 6289 is used to measure the output voltage of the piezoelectric plates. The rectangular quarter-wavelength tube is fabricated by 0.5 inch thick polycarbonate plates. Small notches are fabricated between bottom blocks of the tube. PZT plates were inserted from these notches and clamped by the bottom blocks. Thick sealing caulk is applied between the gaps of the polycarbonates panels to minimize sound leakage.

5. Simulation and experiment results and discussion

In experiment, the amplification factor of the 42 cm quarter-wavelength tube resonator is 97.2 at 199 Hz. In COMSOL simulation, the amplification factor and eigenfrequency at first mode is 100.1 at 198 Hz, which is closed to the experimental results. Single and multiple PZT piezoelectric plates are placed inside the tube resonator to harvest the acoustic energy at 100 dB. Since the resonant behavior of the tube resonator would be changed due to the interaction between the air motion and piezoelectric plates, the frequencies would be swept from 185 to 205 Hz by 1 Hz step size to confirm the maximum plates' output voltage and power in both experiments and simulation.

5.1 Single piezoelectric plate

Fig. 5 shows the simulation and experimental results of one piezoelectric plate output voltage when one plate is moving from the tube inlet to the tube end. When a single piezoelectric plate is located at 5 cm from the tube inlet, the calculated voltage is 1.639 V (at 196 Hz) while 1.433 V (at 199 Hz) was measured from experiments. The output voltage decreases gradually in both experiment and simulation due to the reduction of the acoustic pressure difference Δp. When the PZT plate is placed near the tube inlet where the pressure gradient is at the maximum, the largest output voltage is obtained by a large plate deflection. When the plate is placed near the tube closed end, the small pressure gradient induces a small plate deflection, although the pressure magnitude is at the maximum at the tube closed end.

5.2 Multiple piezoelectric plates

In order to increase the amount of harvested energy, multiple piezoelectric plates have been placed along the centerline of the tube. Piezoelectric plates are placed in the tube starting from the first position *A* near the open inlet to the last position *H* near the closed end as shown in Fig. 6 (a). The spacing between plates along the longitudinal tube axis is 5 cm. Displacements of

the piezoelectric plates reduce gradually from the position *A* to *H*. It is worth to mention that there is a phase shift between maximum plate displacement and sound pressure because of the damping of piezoelectric plates.

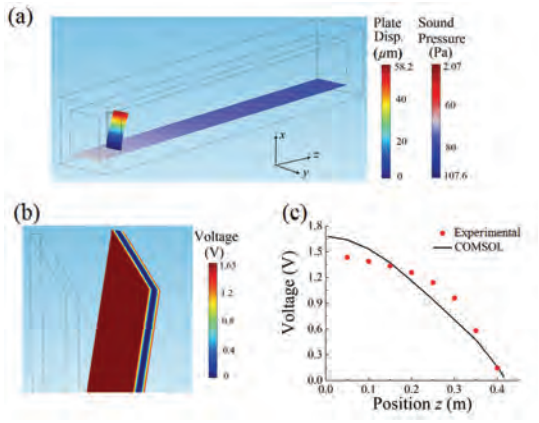

Figure 5. (a) Displacement of a piezoelectric plate located at 5 cm from the tube inlet and the corresponding sound pressure, (b) output voltage of the piezoelectric in the maximum displacement, and (c) experimental and simulation results of output voltage for a single piezoelectric plate when it moves from the tube inlet to the tube end with an incident SPL 100 dB.

In Fig. 6 (b), the total voltage is obtained by the summation of voltage from each plate assuming that all plates are connected electrically in series. From COMSOL simulation, the total output voltage increases to 4.06 V (at 189 Hz) as the number of plates increases until 5 PZT plates are placed in the tube. From experiments, the maximum total voltage of 3.79 V (at 193 Hz) was measured with placing 6 plates. Placing additional plates reduces the total output voltage in both experiment and simulation. This is caused by the alteration of acoustic resonance due to the additional plates near the tube closed end. In order to harvest more acoustic energy available in the resonator, it is desired to place more piezoelectric plates inside the tube. However, the presence of the plates in the tube reduces the acoustic resonant pressure by interrupting the air particle motion along the tube. This effect can also be seen in the first and second bars of Fig. 6 (b). The additional plate at the position *B* has decreased the voltage generated by the plate at *A*.

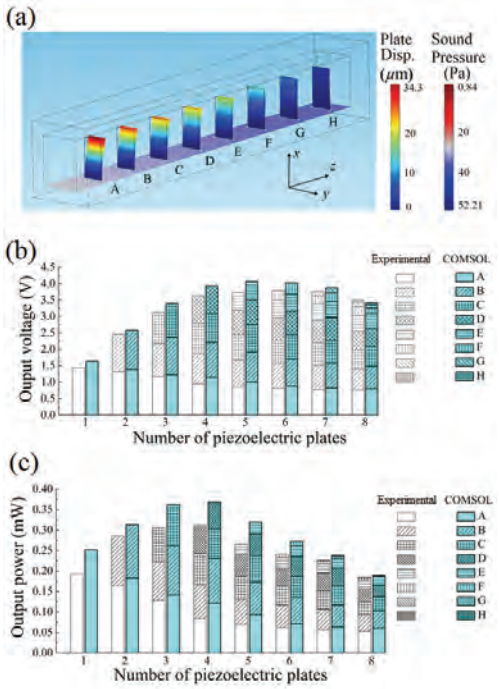

Figure 6. (a) Displacement of 8 piezoelectric plates placed along the centerline of the tube resonator and the corresponding sound pressure, (b) experimental and simulation results of total output voltage and (c) total power with incident SPL of 100 dB.

From the measured voltage for each plate, the total power can be obtained as the summation of power ($\Sigma V_i/R$, i=1, 2,…) from each plate, as shown in Fig. 6 (c). Experiment and simulation reach maximum 0.311 mW (at 190Hz) and 0.369 mW (at 194 Hz) respectively when 4 piezoelectric plates placed at the positions of *A* through *D*. In terms of the total power represented by the summation of V^2/R from each plate, placing more piezoelectric plates also increases the total resistance. Therefore, placing the plates near the closed tube end, where the output voltage is relatively small, reduces the total power due to the increased resistance.

7. Conclusions

A novel and practical acoustic energy harvesting mechanism at low frequency (~200 Hz) using a quarter-wavelength straight-tube resonator with multiple PZT cantilever piezoelectric plates has been studied numerically using COMSOL *multiphysics* 4.3. The simulation results are compared with the experimental data. The amplification ratio at the

first mode of the 42 cm long quarter-wavelength tubes resonator is obtained as 100.1 and 97.2 at 198 and 199 Hz from simulation and experiments, respectively. In simulation, with the incident wave of 100 dB, the single PZT plate near the tube inlet has generated the voltage of 1.64 V (at 196 Hz), which is close to the experimentally measured voltage 1.43 V (at 199 Hz). The voltage gradually decreases as the plate is moved to the tube closed end. In order to increase the total output voltage and power, multiple piezoelectric plates have been placed inside the tube along the centerline of the tube resonator. It has been found that the number of plates to generate the maximum voltage is limited by the interruption of acoustic air particle motion caused by the presence of plates. In simulation, the maximum total output voltage and power generated by multiple piezoelectric plates are 4.06 V at 189 Hz by 5 PZT plates and 0.37 mW at 190 Hz by 4 plates with the incident SPL of 100 dB. The experimental data are 7 % and 19% lower than the simulation results (3.79 V at 193 Hz and 0.31 mW at 194 Hz).

8. References

1. Kamel T., Elfrink R., Renaud M. and Hohlfeld D. *et al.*, Modeling and Characterization of MEMS-based Piezoelectric Harvesting Devices, *J. Micromech. Microeng.*, **20**, 105023 (2010)
2. Renaud M., Fiorini P. and Schaijk R. *et al.*, Harvesting Energy from the Motion of Human Limbs: the Design and Analysis of an Impact -based piezoelectric generator, *Smart Mater. S*truct., **18**, 035001 (2009)
3. Majidi C., Haataja M. and Srolovitz D., Analysis and Design Principles for Shear-mode Piezoelectric Energy Harvesting with ZnO Nanoribbons, *Smart Mater. Struct.*, **19**, 055027 (2010)
4. Wang W. C., Wu L .Y. and Chen L. W. *et al.*, Acoustic Energy Harvesting by Piezoelectric Curved Beams in the Cavity of a Sonic Crystal, *Smart Mater. Struct.*, **19**, 045016 (2010).
5. Zurkinden A., Campanile F. and Martinelli L., Wave Energy Converter through Piezoelectric Polymers, *Proceedings of the COMSOL Users Conference* (*Grenoble*), (2007)
6. Kuehne I., Linden A. and Seidel J. *et al.*, Fluid-Structure Interaction Modeling for an Optimized Design of a Piezoelectric Energy Harvesting MEMS Generator, *Proceedings of the COMSOL Users Conference* (Stuttgart), (2007)
7. Pallapa M., Mohamed A. and Chen A. *et al.*, Modeling and Simulation of a Piezoelectric Micro-Power Generator, *Proceedings of the COMSOL Conference* (*Boston*), (2010)
8. Liu F., Phipps A. and Horowitz S. *et al.*, Acoustic Energy Harvesting Using an Electromechanical Helmholtz Resonator, *J. Acoust. Soc. Am.*, **123**, 1983-90, (2008)
9. Li B. and You J. H., Harvesting Ambient Acoustic Energy Using Acoustic Resonators, *Proceedings of Meetings on Acoustics*, **12** , 065001 (2011)
10. Wang X. D., Song J. H. and Liu J. *et al.*, Direct-current Nanogenerator Driven by Ultrasonic Waves, *Science*, **316**, 102-05 (2007)
11. Ludwigsen D., Jewett C. and Jusczcyk M. *et al.*, Better Understanding of Resonance through Modeling and Visualization, *Proceedings of the COMSOL Users Conference* (*Boston*), (2006)
12. Mahesh N. and Prita N., Experimental And Theoretical Investigation Of Acoustic Metamaterial With Negative Bulk-Modulus, *Proceedings of the COMSOL Users Conference* (*Bangalore*), (2011)
13. Sohn C. H. and J. H. Park, A Comparative Study on Acoustic Damping Induced by Half-wave, Quarter-wave, and Helmholtz Resonators, *Aerosp. Sci. and Technol.*, **15,** 606-14 (2011)
14. Alster M., Improved Calculation of Resonant Frequencies of Helmholtz Resonators, *J. Sound Vib.*, **24**, 63-85 (1972)
15. Roundy S. and Wright P., A Piezoelectric Vibration Based Generator for Wireless Electronics, *Smart. Mater. Struct.*, **13** 1131-42 (2004)